

# Cooling Rate and Fibrous Type Striated Deformations Effects on the Mechanical Properties of Sn– 8.6 wt. % Zn Alloy

F. Abd El-Salam, H.Y. Zahran , Shereen. M. Abdelaziz

**Abstract**— Sn-Zn alloy has been taken as one of the most important lead free solder alloys due to the toxicity and the alpha radiation of lead impurities. The influence of cooling rate on the mechanical and structural properties of Sn – 8.6 wt. % Zn lead free solder alloy was studied. The microstructure of the quenched and slowly cooled samples of Sn – Zn alloy was examined by X – rays analysis and Scanning electron microscopy (SEM). There is an appearance of fibrous type striated deformations on the surfaces of the quenched samples more than those on the surfaces of the slowly cooled samples. The hardening parameters were obtained through stress-strain relations in the temperature range 333-393K for slowly cooled and quenched samples. The quenching samples indicated an improvement in the mechanical properties. The energy activated the rate controlling mechanisms has been calculated and found to be 17.85 and 24.57 kJ/mol for slowly cooled and quenched samples respectively. These values were found to be close to those reported for the grain boundary sliding mechanism in Sn-based alloys.

**Index Terms**— Lead-free solders, Microstructure, SEM, Stress-strain curves, XRD.

## I. INTRODUCTION

The Pb – Sn systems are the most commonly soldering materials used in electronic interconnection, packing and assembling electronic components on printed circuits boards, because of their unique combination of physical, chemical, mechanical properties and low cost. But due to environmental, health concerns and the toxicity of Pb and its compounds, the intensive search for alternative Pb – free solder alloys is in progress [1]. Requirements for the new solder materials include environment friendliness, compatibility with the existing manufacturing line, good wettability, good mechanical and electrical properties, and low cost, among others [2]. Sn – Zn alloys have received much attention because of their good properties as solders for some delicate electronic tools [3].

According to the binary phase diagram of Sn – Zn system, no intermediate phases exist. The absence of an intermediate phase in the Sn – Zn system (given in Fig. 1) is nearly indicated by thermal and microscopic investigations as well as

measurements of various physical properties as a function of composition [4].

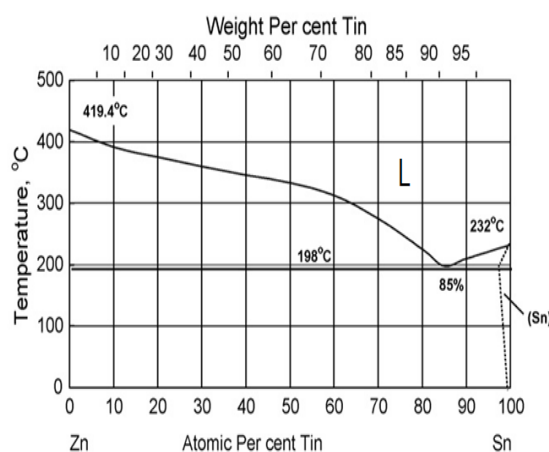


Fig. 1: The equilibrium phase diagram of tin–zinc.

The steady state creep behavior of Sn – 0.5 wt. % Zn and Sn – 9 wt. % Zn alloys had been investigated [5] near the transformation temperature under applied stresses ranging from 12.4 to 16.2 MPa. The activation energies of the steady state creep for both alloys below and above the transformation temperatures were found to characterize the grain boundary and volume self diffusion mechanisms, respectively. Al-Ganainy [6] studied the creep characterization of Sn – 1 wt. % Zn alloy under constant stress in the temperature range from 393K to 453K. Results indicated a transition point at 423K. The effects of 0.5 wt.% Sb and 0.5 wt.% Ni additives on the microstructure and solidification behavior of hypoeutectic Sn – 6.5 wt.% Zn alloy as well as the creep behavior have been investigated [7]. With the addition of Sb and Ni into Sn – 6.5 wt.% Zn alloy significant improvement in creep resistance when compared with the hypoeutectic Sn – 6.5 Zn alloy. There were different Sn-Zn lead free solder systems that have been acknowledged in several studies. But to the best of our knowledge, there are a few studies on the effect of cooling rate treatment on the mechanical properties of Sn – 8.6 wt. % Zn lead free solder alloy.

In the present work we therefore investigated the influence of deformation temperature, cooling rate and striated deformations of fibrous type on the micro structural and mechanical properties of Sn – 8.6 wt.% Zn alloy samples.

F. Abd El-Salam, Physics Department, Faculty of Education, Ain Shams University, P.O. Box 5101, Heliopolis 11771, Roxy, Cairo, Egypt.

H.Y. Zahran , Physics Department, Faculty of Science, King Khalid University, P.O. Box 9004, Abha 61413, Saudi Arabia.

Shereen. M. Abdelaziz , Physics Department, Faculty of Science, Qassim University, P.O. Box 6666, Buraydah 51452, Saudi Arabia.

## II. EXPERIMENTAL PROCEDURES

The Sn – Zn alloy containing 8.6 wt. % Zn was prepared from highly pure Sn and Zn (purity 99.99%) by vacuum melting. Small pieces of these raw materials were melted together in a high purity graphite crucible and then poured into a cast iron mould of dimensions 150 mm x 10 mm x 10 mm and allowed to solidify.

After solidification, the ingot was homogenized at 423K for 24h and slowly cooled to room temperature. The ingot was swaged and cold drawn into:

- (1) Wire samples having 0.7mm diameter and 50mm length for stress – strain measurements.
- (2) Sheets of 0.6mm thick for X-rays diffraction pattern (XRD) and (SEM) examinations.

The samples (wires and sheets) were divided into two groups. Each group contained some wires suitable for the stress – strain tests and some sheets suitable for structure examination. Two groups were annealed at 423K for 2h. One group was rapidly quenched in water (W.Q) at room temperature (300K). The second group was slowly cooled (S.C) to room temperature with a cooling rate  $2 \times 10^{-2}$  K/s.

Stress – strain tests were carried out at the deformation temperature range 333 – 393K in steps of 10K using a conventional tensile testing machine described elsewhere [8].

The deformation temperatures were monitored with a chromelalumel thermocouple held in contact with the test specimen and were maintained within  $\pm 1$  K. The applied stress,  $\sigma$ , was gradually increased (with 30s interval between two successive loadings) and the corresponding elongation was immediately recorded with an accuracy of 0.01 mm. The yield stress,  $\sigma_y$ , is considered as the stress corresponding to the first significant deviation from linearity of the starting part of the stress–strain curve [9]. The maximum stress applied to the sample before fracture was taken as the fracture stress,  $\sigma_f$ , and the corresponding strain is considered to be the fracture strain,  $\epsilon_f$ . The slope of the starting linear part of the stress–strain curve gives the Young's modulus  $Y$ . The coefficient of parabolic work – hardening,  $\chi$ , was obtained [10] as  $\partial\sigma^2/\partial\epsilon$ .

A Shimadzu Lab XRD-6000 with  $\text{CuK}\alpha$  ( $k = 1.5406 \text{ \AA}$ ) radiation and secondary monochromator. XRD tube was operated at voltage = 30 kV and current = 30 mA in the 2 $\theta$  range from 5° to 90°. For scanning electron microscopy investigations, the sheets were etched with an etchant (2 vol.% HCl + 5 vol.% HNO<sub>3</sub> + 93 vol.% C<sub>2</sub>H<sub>5</sub>OH). The surface morphology of the quenched and slowly cooled samples for the studied Sn – Zn alloy was investigated by a scanning electron microscopy (SEM, JSM-6360) with an acceleration voltage = 20 kV.

## III. RESULTS AND DISCUSSION

X-rays diffraction patterns obtained for quenched and slowly cooled samples of Sn – 8.6wt.% Zn alloy are given in Fig. 2. Analysis of X-rays diffraction patterns obtained for the Sn – Zn alloy prepared by normal cast is given as compared to JCDPS card No. 4-0673 for Sn and No. 01-1244 for Zn. It can be observed that the quenched samples (Fig. 2) consist of one phase which is  $\beta$  – Sn matrix. While there is little existence to  $\alpha$ -Zn phase.

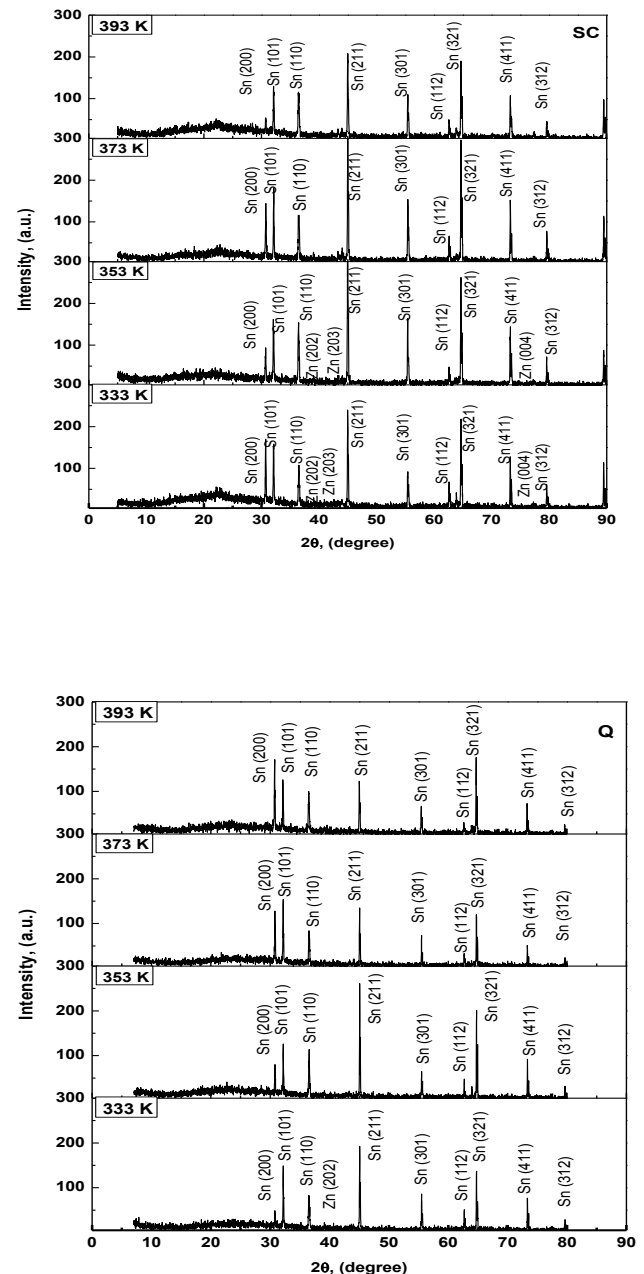


**Fig.2:** X-rays diffraction patterns for the slowly cooled (SC) and quenched (Q) samples of Sn-Zn alloy at different deformation temperatures.

The higher amount of the precipitated Zn in the slowly cooled condition has resulted in more distinct peaks of this phase in its diffraction patterns.

The analysis of the diffraction patterns was carried out, considering that the X-ray diffractometer used is accurately calibrated, and that the diffraction rays breadth  $B$  is affected by the breadth  $B_\eta$  due to the crystallite size, which is obtained from the full width at half maximum intensity (FWHM) in radians and  $B_\epsilon$  due to lattice strain size, and applying the equation [11]:

$$\frac{B \cos \theta}{\lambda} = \frac{1}{\eta} + \frac{2\epsilon \sin \theta}{\lambda}, \quad (1)$$

where  $\theta$  is the peak angle and  $\lambda$  is the wavelength of the used X-rays. From the relation between  $(\beta \cos \theta)/\lambda$  and  $(\sin \theta)/\lambda$  which shows a straight lines, a half of the slope refers to the lattice strain  $\epsilon$ , the inverse number of the intercept at the ordinates (y – axis) gives the average crystallite size  $\eta$  (Å). To have more information about structure characteristics of the studied alloy the average dislocation density ( $\rho=1/\eta^2$ ) can be calculated. The deformation temperature dependence of the average crystallite size  $\eta$  lattice strain  $\epsilon$  and dislocation density  $\rho$  is given in Figs. 3 (a-c). It should be noted that increasing deformation temperature for both groups of the tested samples (SC and Q) increased the values of the crystallite size  $\eta$  but decreased the values of dislocations density  $\rho$  and lattice strain  $\epsilon$ .

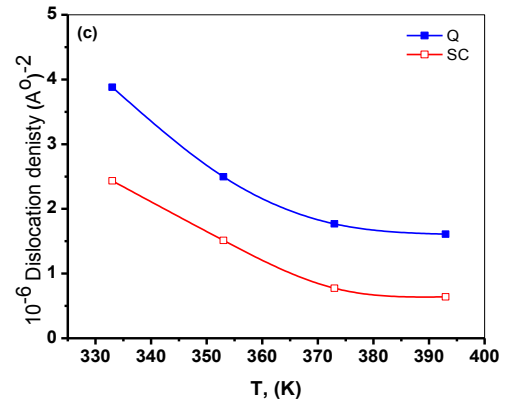
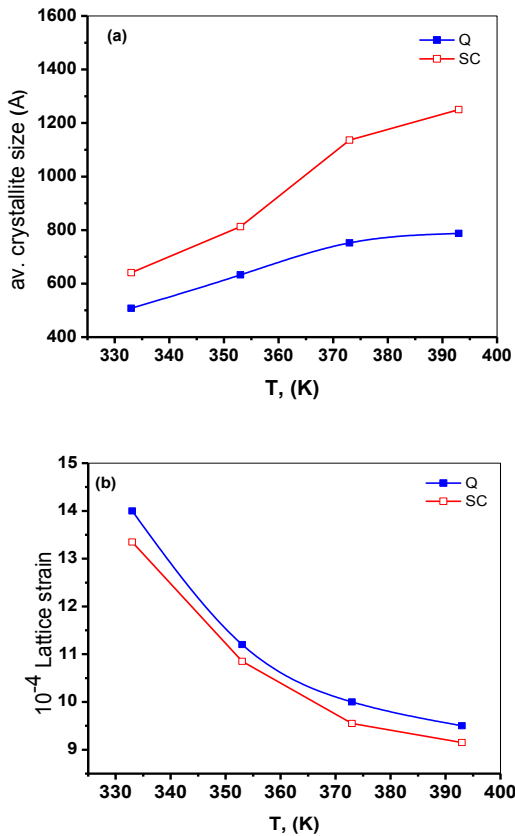


**Fig. 3(a-c):** The temperature dependence of (a) average crystallite size  $\eta$ , (b) lattice strain  $\epsilon$  and (c) dislocation density ( $\rho=1/\eta^2$ ) for the slowly cooled (SC) and the quenched (Q) samples of Sn–Zn alloy.

Increasing deformation temperature enhances the grain boundary migration and results in the increase of  $\beta$ -Sn grain size and the decrease in lattice strain and dislocation density for SC and Q samples. It is also observed that the values of the crystallite size for slowly cooled samples are higher than those for quenched samples. This is due to the tendency of Zn atoms to segregate on deformed grain boundaries [3] and this will retard softening and decreases the grain size of Sn (as shown in Fig. 4).

The microstructure of the slowly cooled and quenched samples for the studied solder alloy at 333K and 393K is shown in Figs. 4 (a, b) and Figs. 4 (c, d) respectively. It was observed that there were two phases, namely; the gray  $\beta$ -Sn and dark Zn-rich phases. The cooling rate significantly affects the microstructure of the cast Sn–Zn alloy.

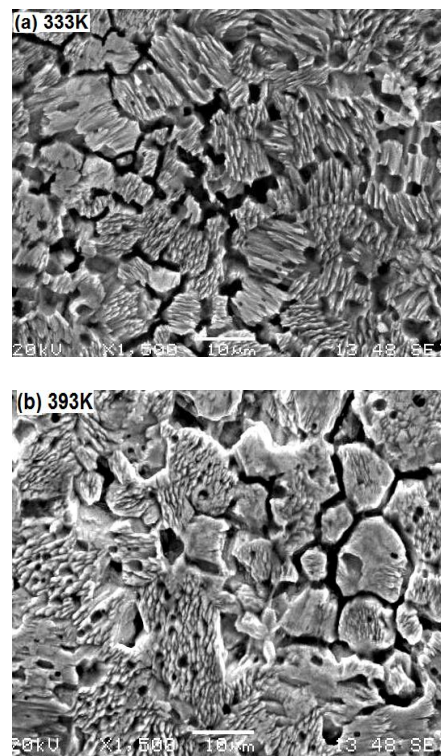


**Fig. 4:** SEM micrographs for (a, b) the slowly cooled (SC) samples of Sn–Zn alloy at 333K and 393K.

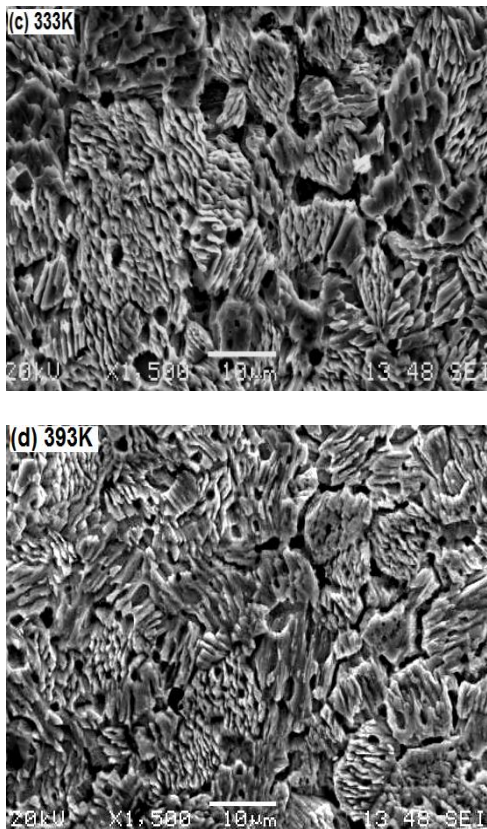


**Fig. 4:** SEM micrographs (c, d) the quenched (Q) samples of Sn–Zn alloy at 333K and 393K.

Quenched sample has a refined structures and little existence of Zn phases but the slowly cooled sample has a network of precipitated Zn in the Sn matrix.

Due to the fast cooling rate, the striated deformation feature could be found on the quenched specimen surface at both deformation temperatures 333K and 393K and it could be identified as the fibrous type in Sn–Zn eutectic. On the other hand there was little appearance for these fibrous type of striated deformations on the surfaces of the slowly cooled specimens. These deformations didn't form easily because of the uniformly distribution of Zn in  $\beta$ -Sn matrix. This also gave rise to the increases in dislocation mobility. Fibrous type of striated deformations on the surface of the tested samples decreased with increasing deformation temperature from 333K to 393K for both slowly cooled and quenched samples.

The stress – strain curves for both slowly cooled and quenched Sn – 8.6 wt.% Zn samples under different deformation temperature ranging from 333 to 393K are illustrated in Figs. 5 (a, b). It is observed from Fig. 5 that these curves are sensitive to the heat treatment prior to the tensile test and the deformation temperature. The levels of the curves shifted towards lower flow stresses and higher ductility with increasing deformation temperature. The slowly cooled samples were softer than the quenched samples. The softening behavior of the deformed samples observed with increasing deformation temperatures is revealed from the decreased values in the following hardening parameters: a) the yield stress  $\sigma_y$ , b) fracture stress

$\sigma_f$ , c) Young's modulus  $Y$ , d) the work hardening coefficient  $\chi$  obtained and e) the fracture time  $t_f$  (time of a full stress – strain run till fracture). On the other hand, the softening parameters, i) the fracture strain  $\epsilon_f$ , and j) the dislocation slip distance  $L$ , increased with increasing deformation temperature.

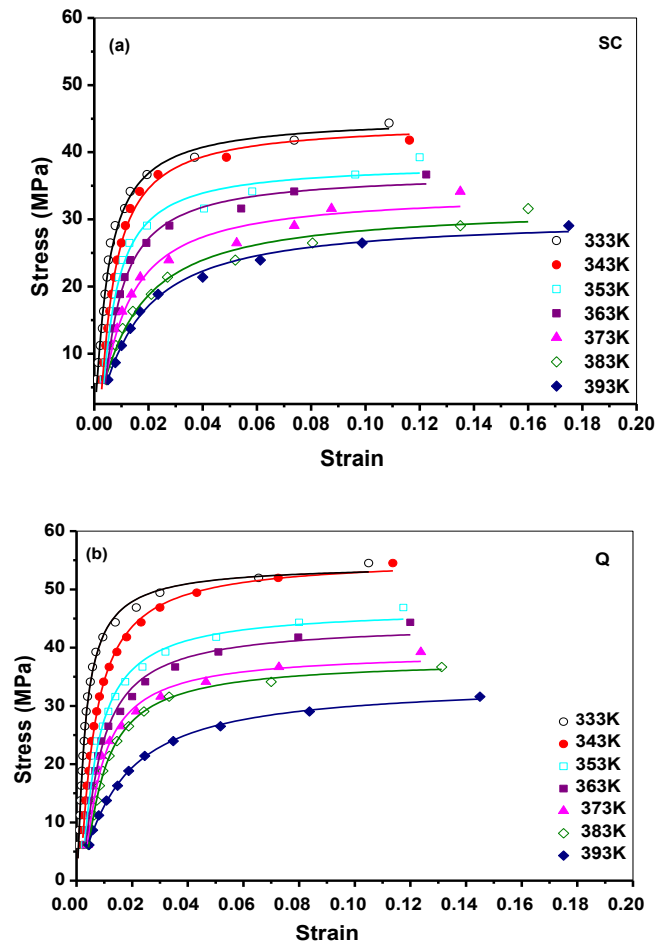


**Fig. 5:** Stress –strain curves at different deformation temperatures for (a) the slowly cooled (SC) samples and (b) the quenched (Q) samples of Sn–Zn alloy.

The temperature dependence of the yield stress  $\sigma_y$  and fracture stress  $\sigma_f$  in Fig. 6(a, b), work hardening coefficient  $\chi$  obtained as  $\partial\sigma^2/\partial\epsilon$ , (Fig. 7), the stress per unit strain  $\partial\sigma/\partial\epsilon$  (Young's modulus) (Fig. 8), fracture strain,  $\epsilon_f$ , (Fig. 9) and the dislocation slip distance,  $L$ , (Fig. 10) calculated from Mott's model [12] given as  $\chi = \partial\sigma^2/\partial\epsilon = G^2b/2\pi^2L$ , where  $G$  is the shear modulus of the material, and  $b$  is the Burger's vector.

The nature and mode of interaction of the existing defects and the alloy components is controlled and modified by the internal state of the alloy. The effect of temperature on the measured parameters may lead to either hardening or softening depending mainly on the internal state. The temperature dependence of the observed variations in the measured parameters proves that they are structure sensitive parameters.

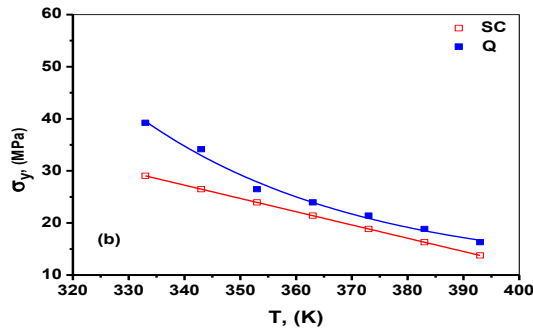
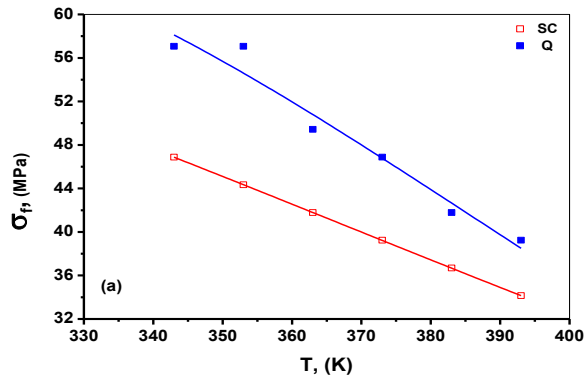


Fig. 6: The temperature dependence of (a)  $\sigma_f$ , (b)  $\sigma_y$ , for slowly cooled (SC) and quenched (Q) samples.

In general, raising temperature makes easier dislocations overcome obstacles in the matrix and so their average slip distance increase and Young's modulus  $Y$  decreases. In the cast Sn – Zn slowly cooled alloy, the interaction seems to improve the order in the alloy structure with the components becoming ordered by annihilation of some defects and modifying the existing dislocation system, so that on increasing the deformation temperature the slowly cooled alloy shows its higher observed softening over that of the quenched alloy samples.

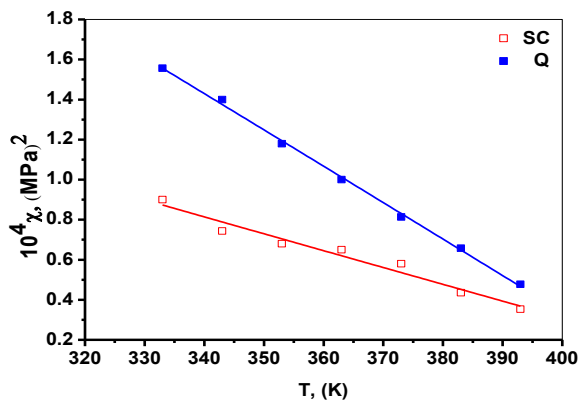


Fig. 7: The temperature dependence of  $\chi$  for SC and Q samples.

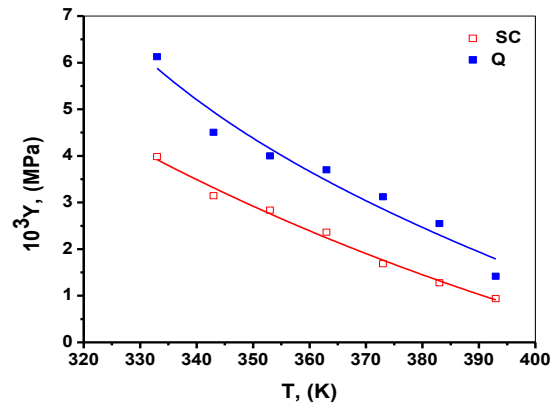


Fig. 8: The temperature dependence of Young's modulus for SC and Q samples.

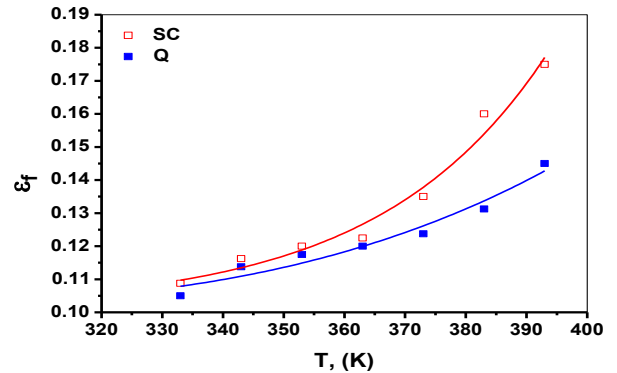


Fig. 9: The temperature dependence of fracture strain,  $\epsilon_f$ , for SC and Q samples.

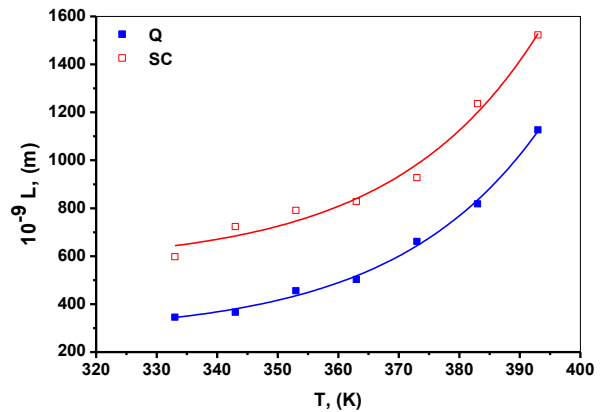


Fig. 10: The temperature dependence of dislocation slip distance for SC and Q samples.

The observed low values of the hardening parameters and also the higher softening parameters values of the slowly cooled samples in comparison to those of the quenched samples, is due to the high concentration of point defects introduced by the quenching technique for the quenched samples [13].

Besides, the observed larger grain boundary area and Fibrous type of striated deformations in the quenched samples (shown in Figs. 4(c,d) which hinder the motion of dislocations and needs high amounts of energy to cause the

higher values of the hardening parameters for these samples than those of the slowly cooled samples, which are larger grain size, smaller grain boundary area and have little fibrous type of striated deformations on their surfaces (shown in Figs. 4(a,b).

In metals and alloys deformed in tension, it is easy for dislocations to pile-up near grain boundaries [14] and easy for vacancies to form and then gather into clusters. The internal stresses will supply the dislocations piled-up with the energy required to climb and surpass these barriers, thus increasing the tensile strain. This softening might also be due to the formation of dislocations with their distribution aligned with the direction of tension during tensile test making them have maximum mobility in the direction of tension contributing to the overall strain.

The temperature dependence of the mechanical parameters obtained from the stress – strain curves (Fig. 5), points in general to the softening behavior acquired by all the tested samples with increasing deformation temperature, it is clear from Fig. 4 that the fibrous type of striated deformations on the surface of the tested samples decreased with increasing deformation temperature from 333K to 393K for both slowly cooled and quenched samples.

But the hardening parameters for the quenched samples are higher than those for slowly cooled samples, Figs. (6-10). This may be due to the induced quenching defects. The thermally induced in-homogeneity in composition and mass distribution, and the activated interaction of all these existing defects with each other and with the solute atoms are the main factors which control the observed variations in the obtained data.

The increased density of point defects produced by quenching from high temperature and the increase in dislocations density due to plastic deformation lead to a certain hardening level due to the cutting of the moving and stationary dislocations and mutual annihilation of defects at higher temperatures. Besides, the efficiency of migration of point defects to dislocations and the probability of the formation of unstable mobile clusters of point defects in the matrix. Also the grain refining effect of Zn contributes to the improvement of the mechanical properties of the quenched samples [3].

Generally, cooling rate also affects the mechanical properties of the cast Sn–Zn alloy. Quenched samples, Figs. 4(c,d), with refined structures are harder than the slowly cooled samples, Figs. 4(a,b) having a network of precipitated Zn in the Sn matrix. This is believed to be due to the strengthening effects of Zn in the Sn matrix, compensating for the finer grain size of the Q samples which tends to act in the opposite direction. As it is known that the deformation mechanisms in the particle-strengthened or multiphase eutectic structures [7] of the Pb free alloys may be similar to those observed in pure tin, but operate at higher stress than in pure Sn.

It was reported [11] that the variation of hardness ( $H$ ) with temperature is similar to the variation of yield stress ( $\sigma_y$ ) with temperature since hardness is intimately related to the yield stress and typically  $H= 3\sigma_y$  in bulk metals, so the hardness values can be obtained from yield stress values for slowly

cooled and quenched samples at different deformation temperatures. Also, the variation of hardness with temperature was proposed as [15]:

$$H=H_o \exp(-\alpha T), \tag{2}$$

where  $H_o$  is the hardness at 0K, or the intrinsic hardness, and  $\alpha$  is the softening coefficient [16]. Applying this equation, from the relation between  $\ln H$  and  $T$  given in Fig.11, the softening coefficient  $\alpha$  was obtained for slowly cooled and quenched samples. Its value did not change too much, it was (0.012) for slowly cooled samples and (0.01) for quenched samples.

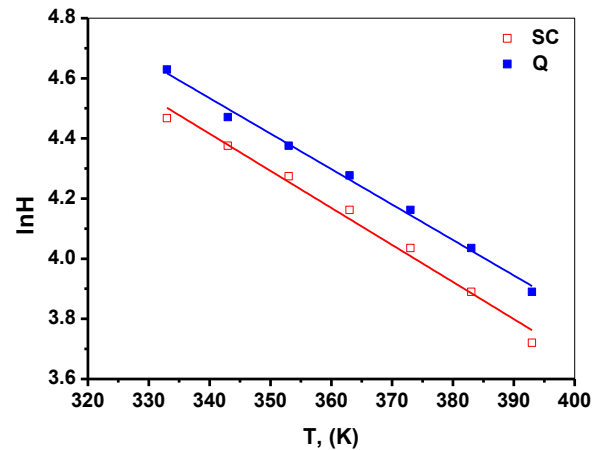


Fig. 11: The plot of  $\ln H$  versus deformation temperature,  $T$ , for SC and Q samples.

The tensile behavior of the slowly cooled or the quenched samples depends mainly on the nature of the interaction between the type of the dispersed phase and glide dislocations. The increased hardness of the quenched samples, ( $\beta$  - Sn matrix) [13], could be due to the high vacancy concentration existing in the quenched samples, the migration of solute - vacancy pairs towards dislocations, and the formation of solute atmospheres around them with the result in the density of the mobile lattice defects [12,17]. During the isothermal deformation of the quenched samples, the strengthening taking place may be due to the nucleation and growth of the precipitating phase from the solid solution, this comprises the dissolution of the solids [13]. The increased hardness observed dominate in the results of the quenched samples compared with the lower hardness results of the slowly cooled samples. This may be rendered to the strength variation of the phases existing at low temperature during deformation at temperatures above room temperature. The rate of aging increases with increasing temperature, whereas the maximum strength achieved is progressively reduced for higher working temperatures which enhance the dissolution of the incoherent  $\alpha$  - Zn phase atoms in the  $\beta$ - Sn matrix. The increased recovery of the vacancy – type defects enhances the rate of diffusion of solute atoms. Hence, for a given alloy composition the large particles will be less effective in holding up dislocations or inhibiting slip. This leads to a strength fall and a ductile state with reduced flow stress.

According to Semenchenko [18] the extent to which the impurity will segregate at the boundaries can be estimated

from the difference between the general moment  $m(=Ze/r)$  of the impurity atom and the moment  $m_o(=Ze/r_o)$  of the parent matrix, where  $Z$  is the atomic number,  $e$  is the electronic charge and  $r$  and  $r_o$  are the radii of the impurity and matrix atoms, respectively. If the difference  $\Delta m = m_o - m$  is positive, then the impurity atoms will be adsorbed on the grain boundaries. If  $\Delta m$  is not positive (is negative), then the impurity atoms will migrate away from the boundaries to the interior of the grains.  $\Delta m$  for the studied alloy (Sn – Zn) will be positive so the impurity atoms (Zn atoms) will be concentrated at the grain boundaries of Sn - matrix.

The work hardening parameter,  $\chi$ , was assumed to vary with the deformation temperature,  $T$ , according to an Arrhenius-type relation [19] of the form,

$$Q = (\partial \ln \chi / \partial (10^3/T)) \quad (3)$$

where  $Q$  is the activation energy (kJ/mol). From the plots of  $\ln \chi$  versus  $1000/T$  given in Fig. 12, the calculated values of  $Q$  are (17.8 kJ/mol) for the slowly cooled samples and (24.5 kJ/mol) for the quenched samples.

It is clear from these values of activation energy that the activation energy for quenched samples are higher than those for slowly cooled samples. But they indicated that there is low variation in the energy activating the rate controlling mechanisms for slowly cooled and quenched samples of Sn - Zn alloy. They were found to be close to those reported for the grain boundary sliding mechanism in Sn-based alloys [20-22].

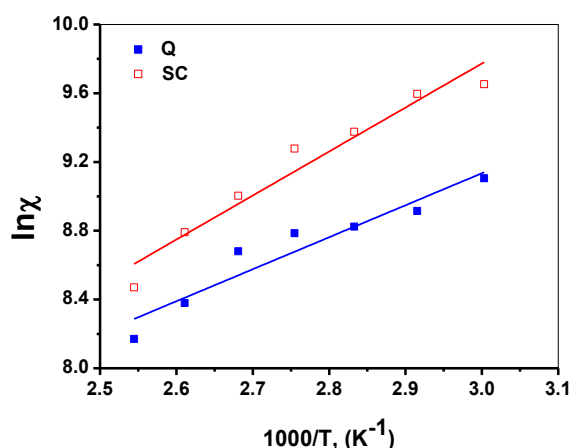


Fig. 12: The plot of  $\ln \chi$  versus  $1000/T$  for SC and Q samples.

#### IV. CONCLUSION

The mechanical properties for slowly cooled and quenched samples of Sn -8.6 wt.% Zn based lead-free solder alloy have been studied through stress – strain measurements in the deformation temperature range (333 – 393K) and it can be concluded that:

1- Cooling rate significantly affects the microstructure and mechanical properties of the cast Sn–Zn alloy. Quenched samples with refined structures are harder than the slowly cooled samples having a network of precipitated Zn in the Sn matrix. This is believed to be due to the

strengthening effects of Zn in the Sn matrix, compensating for the finer grain size of the Q samples which tends to act in the opposite direction.

2- The softening behavior of the quenched and slowly cooled samples observed with increasing deformation temperatures is revealed from the decreased values in the hardening parameters and the increased values in the softening parameters.

3- The data of the stress – strain measurements for the quenched samples showed more enhancement in mechanical properties than the slowly cooled samples, this may be due to the induced quenching defects.

4- The striated deformations observed on the quenched specimens surfaces at both deformation temperatures 333K and 393K are more than those observed on the slowly cooled specimens surfaces and they could be identified as the fibrous type in Sn–Zn eutectic.

5- The activation energy for quenched samples are higher than those for slowly cooled samples and they were found to be close to those reported for the grain boundary sliding mechanism in Sn-based alloys.

#### REFERENCES

- [1] Y. S. Kim, K. S. Kim, C. W. Hwang, K. Sugauma, J. Alloys and Compounds 352 (2003) 237.
- [2] A. F. Abd El-Rehim, J. Mater. Sci. 43 (2008) 1444.
- [3] F. Abd El-Salam, A. M. Abd El- Khalek, R. H. Nada, Mater. Sci. Eng. A 460 (2007) 14.
- [4] S. Y. Eysa, MSc Thesis, Ain Shams Univ., Cairo, Egypt (1995) 62.
- [5] M. S. Sakr, A. Z. Mohamed, A. A. El-Daly, A. M. Abdel-Daiem, A. H. Bassyoni, Egypt J. Solids 13 (1990) 34.
- [6] G. S. Al-Ganainy, Phy. Stat. Sol. (a) 169 (1998) 217.
- [7] A. A. El-Daly, A. E. Hammad, G. S. Al-Ganainy, A. A. Ibrahim, Mater. & Des. 56 (2014) 594.
- [8] H. S. M. Sayed, MSc Thesis, Ain Shams Univ., Cairo, Egypt (2011) 47.
- [9] M. S. Sakr, A. A. El-Shazly, M. M. Mostafa, H. A. El-Sayed, Czech. J. Phys. 40 (1990) 1267.
- [10] M. A. Mahmoud, M. Sobhy, A. F. Abd El-Rehim, R. M. Abdel Rahman, Physica B 405 (2010) 3616.
- [11] H. Y. Zahran, MSc Thesis, Ain Shams Univ., Cairo, Egypt (2006) 32.
- [12] N. F. Mott, Trans. Metal. Soc. AIME 218 (1960) 6.
- [13] F. Abd El-Salam, R. H. Nada, A. M. Abd El- Khalek, Physica B 292 (2000) 71.
- [14] K. Qingping, W. Xing, Ni. Qunhui, Acta Physica Sinica (1985) 973.
- [15] B. M. Kramer, P. K. Judd, J. Vac. Sci. Tech A 3 (1985) 2439.
- [16] G. Sharma, R. V. Ramanujan, T. R. G. Kuty, G. P. Tiwari, Mater. Sci. Eng. A 278 (2000) 106.
- [17] M. M. Mostafa, R. H. Nada, F. Abd El- Salam, Phys. Stat. Sol. A 143 (1994) 297.
- [18] V. K. Semenchenko, Surface phenomena in metals and alloys, Pergamon, London, (1961).
- [19] F. Fahim, MSc Thesis, Ain Shams Univ., Cairo, Egypt (2013) 70.
- [20] A. A. El-Daly. Phys. Stat. Sol. A 200 (2003) 333.
- [21] A. A. El-Daly. Phys. Stat. Sol. A 201 (2004) 2035.
- [22] A. Fawzy, Mater. Charac. 58 (2007) 323.